ADSORPTION OF ANIONIC DYES FROM AQUEOUS SOLUTIONS BY CALCINED AND UNCALCINED Mg/Al LAYERED DOUBLE HYDROXIDE

(Penjerapan Pewarna Ionik daripada Larutan Akues Menggunakan Mg/Al Dwi-Hidroksida Berlapis Berkalsin dan Tanpa Kalsin)

Siti Mariam Sumari*, Zaini Hamzah, Nesamalar Kantasamy

Faculty of Applied Sciences,
Universiti Teknologi MARA, 40450 Shah Alam, Selangor, Malaysia

*Corresponding author: sms21vic@gmail.com

Abstract

The uptake of Acid Blue 29 (AB29), Reactive Orange 16 (RO16) and Reactive Red 120 (RR120) from aqueous solutions by calcined (CLDH) and uncalcined Mg/Al layered double hydroxide (LDH) has been investigated. The adsorption process was conducted in a batch mode at 25 °C. Anionic dye removal was more efficient using the CLDH rather than LDH. The adsorption process by CLDH involved reconstruction and hydration of the calcined LDH and intercalation of AB29, RO16 and RR120. Physical characterization using X-Ray Diffraction (XRD), Scanning Electron Microscopy (SEM) and Fourier Transform Infrared (FTIR) were used to ascertain the 'memory effect' phenomenon that is structural reconstruction to regain its original LDH after rehydration. To gain insight into the mechanism of adsorption by CLDH, the pseudo-first order (PFO) and pseudo-second order (PSO) and intraparticle diffusion (IPD) kinetic models were used to analyse experimental data. Based on the correlation coefficient (R^2), the PSO has better fitting ($R^2 = 0.987 – 1.00$) compared to PFO ($R^2 = 0.867 –0.990$). Furthermore the values of maximum adsorption capacity, (q_e) calculated from PSO model are consistent with the experimental q_e indicating that the experimental kinetic data for AB29, RO16 and RR120 adsorption by CLDH are suitable for this model. Recycling of the adsorbent, in cycles of calcination-reconstruction process promised a possibility of regeneration of CLDH.

Keywords: calcined, adsorption capacity, reconstruction, memory effect, regeneration

Abstrak

Penyingkiran pewarna Acid Blue 29 (AB29), Reactive Orange 16 (RO16) dan Reactive Red 120 (RR120) daripada larutan akues menggunakan Mg/Al dwi-hidroksida berlapis berkalsin (CLDH) dan tanpa kalsin (LDH) telah dilakukan menggunakan kaedah berkelompok pada suhu 25 °C. Penjerapan bahan pewarna menggunakan CLDH didapati lebih berkesan berbanding LDH. Penjerapan bahan pewarna oleh CLDH berlaku melibatkan proses penghidratan dan penstrukturan semula CLDH dan juga apitan AB29, RO16 dan RR120. Pencirian fizikal pada bahan penjerap yang diperolehi dengan menggunakan kaedah Pembelauan Sinar-X (XRD), Mikroskopi Imbasan Elektron (SEM) dan Spektroskopi Inframerah Transformasi Fourier (FTIR) telah digunakan untuk mengenalpasti fenomena 'kesan memori', iaitu proses penstrukturan semula kepada LDH selepas berlaku penghidratan. Cerapan lebih lanjut mengenai mekanisme proses penjerapan ini, model-model kinetik pseudo tertib pertama (PFO), pseudo tertib kedua (PSO) dan resapan intrapartikel (IPD) telah digunakan untuk menganalisis data ujian. Berdasarkan nilai pekali korelasi (R^2), model PSO didapati lebih sesuai ($R^2 = 0.99 – 1.00$) berbanding PFO ($R^2 = 0.85 – 0.99$). Fakta ini diperkukuhkan lagi dengan nilai kapasiti penjerapan maksimum, (q_e) hasil pengiraan menggunakan PSO yang didapati konsisten dengan q_e ujian ($q_{e, expt.}$) untuk AB29, RO16 dan RR120. Kitaran semula bahan penjerap melalui beberapa siri kitaran pengkalsinan-penstrukturan semula juga didapati dapat menjanjikan penjanaan semula CLDH.

Kata kunci: berkalsin, kapasiti penjerap, penstrukturan semula, kesan memori, penjanaan semula

Introduction

Dyehouse effluent usually contain various types of dye classes such as azo, anthraquinone, triphenylmethane,etc. Most of them are synthetic aromatic benzenoid compounds with potential toxic, mutagenic and carcinogenic properties, endangering human health and environment [1]. Generally, they are difficult to treat by conventional water treatment as they are structurally stable to biodegradation [2, 3].The most efficient colour removal from aqueous solution has been attributed to adsorption, which largely employs activated carbon (AC) as adsorbent. Since AC is commercially costly for large scale production and difficult to regenerate, alternative adsorbents are being sought. A positively charged anionic clay known as layered double hydroxide (LDH), with an empirical formula $[M^{II}_{1-x}M^{III}_{x}(OH)_2]^{x+}[A^{n-}_{x/n}\cdot mH_2O]^{x-}$, where M^{II} = Zn, Mg, Co, Ni and M^{III} = Al, Fe, Cr, Ga, etc., A^{n-} = CO_3^{2-}, NO_3^{-}, Cl^-, SO_4^{2-} [4, 5] is known for its versatile applications as well as excellent adsorbent for anionic species in aqueous solution.

Calcination of LDHs at temperature 400 – 700 °C can decompose LDH containing carbonate or nitrate to   release CO_2 or NO_x gas with end products containing a solid mixture of Mg–Al oxide, which can revert to the original structure (reconstruction) of LDH upon rehydration [1, 6]. This phenomenon, well known as 'memory effect' was responsible for enhanced uptake of anionic dye removal by CLDH in comparison to its precursor LDH. The objective of this study is to investigate the kinetic behaviour of AB29, RO16 and RR120 adsorption by CLDH in comparison to its precursor LDH, while at the same time to assess the possibility of regeneration of the adsorbent. Kinetic parameters are important pre-requisites for eventual design of water treatment processes employing the use of adsorbents such as LDH/CLDH. XRD, FTIR and SEM were used to characterize the adsorbents before and after dye adsorption by CLDH. Kinetic models, Lagergren's pseudo-first order [7], Ho's pseudo-second order [8] and intraparticle diffusion [9] were used to gain understanding of the adsorption mechanism of by CLDH.

Therefore, desorption or calcination study was undertaken to evaluate the prospect of regeneration and reuse of the adsorbent.

Materials and Methods
Preparation of adsorbent LDH by co-precipitation method

Synthesis of layered double hydroxide (LDH) of the formula, $[M^{2+}_{1-x}M^{3+}_{x}(OH)_2]A^{n-}_{x/n}.mH_2O$ with M^{2+} = Mg^{2+}, M^{3+}=Al^{3+} and interlayer anion, A^{n-} = NO_3^{-} was conducted by coprecipitation procedure followed by hydrothermal treatment as outlined by several authors [10 – 12], with slight modification. A solution of $Mg(NO_3)_2.6H_2O$ and $Al(NO_3)_3.9H_2O$ with molar ratio of Mg/Al:4/1 were allowed to mix with 1M NaOH by drop wise addition of NaOH at a rate of 1 mL/min, stirring the mixture all the time using a magnetic stirrer, while keeping N_2 gas bubbling in the solution mixture throughout the coprecipitation process. This was to minimize the inclusion of CO_2 in the solution. The N_2 addition was allowed to continue until the solution's pH reading reached 10.0 ± 0.5 in a 1L beaker. The resulting heavy slurry was poured into stoppered glass bottles, and then aged in a thermostated oil bath shaker operating at 70 °C, 100 rpm for 24 hours duration. Once the resulting white precipitate was cooled, it was washed several times with distilled water until the pH reached 7 – 8, to get rid of excess alkali, after which the solid was separated out by vacuum filtration. The final white solid, named layered double hydroxide (LDH) was dried (80 °C, 24 hours) before being ground and sieved.

Preparation of calcined LDH

Calcination of the synthesized LDH was carried out by heating LDH at a designated temperature (100, 200, 300, 400, 500, 600 and 700 °C) in a furnace (Lenton, UK) for 8 hours. The calcined product (henceforth referred to as CLDH100, CLDH200, etc.) was stored in a desiccator prior to characterization and adsorption studies. The calcined product (CLDHs) were subjected to contact time experiment to study which CLDH (CLDH100, CLDH200, CLDH300, etc.) gave the highest percentage of dye removal and adsorption capacity, and consequently selected for adsorption by CLDH in comparison with its precursor LDH. In carrying out this experiment for a particular dye, the dosage and volume (*W/V*) were kept constant.

Preparation of adsorbates

Aqueous stock solutions (1000 mg/L) of RR120, RO16 and AB29 were prepared, from which diluted solutions were obtained for batch adsorption analysis. The chemical structures and physical properties of the three dyes are shown in Figure 1.

C.I Name	Acid blue 29 (AB29)
C.I No	20460
Formula Weight	616.49
Class	Diazo
λ_{max}	602 nm
Mol. Formula	$C_{22}H_{14}N_6Na_2O_9S$
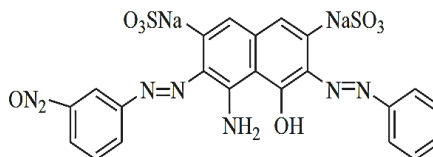
C.I Name	Reactive Orange 16
C.I No	17757
Formula Weight	617.53
Class	Azo
λ_{max}	494 nm
Mol. Formula	$C_{20}H_{17}N_3Na_2O_{11}S$
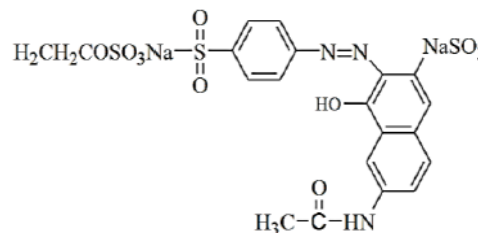
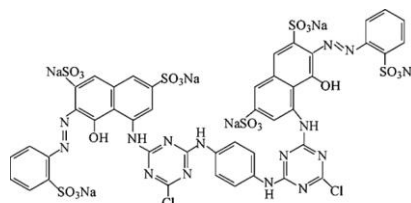|	
C.I Name	Reactive Red 120
C.I No	25810
Formula Weight	1469.43
Class	Azo, Triazine
λ_{max}	532 nm
Mol. Formula	$C_{44}H_{24}Cl_2N_{14}Na_6O_{20}S$

Figure 1. Chemical structures and physical properties of AB29, RO16 and RR120

Adsorption by calcined LDH (CLDH) and uncalcined LDH

The adsorption of AB29, RO16 and RR120 by LDH and CLDH was conducted in a batch mode in duplicates using initial concentration ranging from 50 to 100 mg/L with a constant dose of 0.2 g/L adsorbent at 25 ± 1°C in a thermostated water bath shaker, operating at 100 rpm. Since a previous separate experiment had shown that maximum removal for anionic and acidic dyes occurred at mild acidic pH, the batch adsorption of dyes under study was conducted at the pH of natural solutions without pH adjustment since the dyes are weakly acidic (5.6 – 6.6). This would be cost saving procedure since no extra cost for chemicals would be necessary. At the end of predetermined contact time (0 – 1440 min), the solution was filtered using 0.45 µm cellulose nitrate syringe filter (Whatman) so the remaining dye left in the solution can be measured using UV-Vis spectrophotometer (Secoman UVIKON SL/XS (M8307) at the wavelength of maximum absorption of each dye (Figure 1).

Adsorption data obtained were analysed for amount of dye adsorbed by the LDH and CLDH in terms of adsorption capacity (q_t, mg/g) and percentage dye removal (%) using the Equation (1) and (2), respectively

$$\text{Adsorption capacity, } q_t \text{ (mg/g)} = \frac{(C_0 - C_t)V}{W} \tag{1}$$

Dye removal (%) $= \frac{(C_0 - C_t)}{C_0}$ x 100   (2)

where, q_t is adsorption capacity in mg/g, C_o and C_t are initial and final dye concentrations (mg/L) after treatment for certain period of time, t; V is the volume of each dye solution (L) and W is the weight of adsorbent (g). At equilibrium time t_e, $q_t=q_e$.

Kinetic modeling
The data obtained from these experiments were used to evaluate the kinetic parameters. To gain insight into the mechanism of adsorption by LDH and CLDH, pseudo-first order (PFO) (Equation 3a), pseudo-second order (PSO) (Equation 4a) and intra-particle diffusion models (IPD) (Equation 5) were applied.

Pseudo-first order (PFO) model
The linear expression based on Lagergren's PFO rate equation [7] is represented by Eq. (3a):

$$\log(q_e - q_t) = \log q_e - \frac{k_1 t}{2.303}$$ (3a)

The initial rate h_1 (mg/g. min), at t=0 is defined by the following expression:

$$h_1 = k_1 q_e$$ (3b)

A linear plot of $\log(q_e - q_t)$ versus t enables the determination of k_1 (1/min) and q_e from the gradient and intercept of the plot.

Pseudo-second order (PSO) model
The linear expression for Ho's PSO rate equation [8] is represented by Equation (4a):

$$\frac{t}{q_t} = \frac{1}{k_2 q_e^2} + \frac{t}{q_e}$$ (4a)

The initial rate h_2 (mg/g. min), at t=0 is defined by the following equation:

$$h_1 = k_2 q_e^2$$ (4b)

A linear plot of t/q_t versus t enables the determination of k_2 (g/mg.min) and q_e, from the intercept and the slope.

Intraparticle diffusion (IPD) model
The possibility of IPD resistance affecting adsorption was explored by using the Weber-Morris IPD model [9] is represented by Equation (5):

$$q_t = k_p t^{0.5} + C$$ (5)

where k_p(g/mg.min) is the intraparticle diffusion rate constant and C. By plotting q_t versus $t^{0.5}$, the values of k_p was calculated from the slope. The value of constant C can be found from the intercept and is a measure of the thickness of boundary layer. Hence, the higher value of C, the greater the effect of boundary layer [13]. Based on IPD theory, the plot is linear if intraparticle diffusion is involved in the adsorption process. Additionally, if these lines pass through the origin then intra particle diffusion is the rate controlling step [14,15].

Desorption and regeneration
The residue after initial adsorption (0 cycle) by CLDH was thermally treated at its calcination temperature and the final product (regenerated CLDH) was again subjected to dye adsorption (1st cycle). This process was repeated until

the 4th cycle when the percentage removal of dye became less than 25 – 30 %. The reusability of regenerated adsorbent was based on percentage dye removal calculated for each cycle using Equation 2.

Characterization
Powder X-Ray Diffraction (PXRD) is a technique used to characterize the crystallite size (grain size), crystallographic structure, and the preferred orientation in polycrystalline or powdered solid samples. The X-ray diffraction (XRD) patterns of LDHs and CLDHs before and after adsorption were recorded using a PanAlytical (Germany) diffractometer under the following conditions: 40 kV, 25 mA, Ni-filtered Cu-Kα radiation ($\lambda = 1.542$ Å) and scanning rate of 2θ/min in the range of 10 – 70 °C. The XRD patterns enable the elucidation of basal spacings (d-spacings) of LDHs and CLDHs at pre or post adsorption of dye and give some indications of any change in crystallographic structure. Microstructural examination of LDH and CLDH was carried out using a Carl Zeiss SMT-Supra 40VP (Germany) scanning electron microscope (SEM) to study surface morphologies. The specific surface area of LDH and CLDH was obtained from adsorption/desorption isotherm of liquid N_2 at -196 °C following the standard Brunauer, Emmett and Teller (BET) method using using Micromeritics surface area analyser (USA).

Results and Discussion
Calcination temperature of Mg/Al LDH
Figure 2 shows the results based on a preliminary investigation on percentage of dye removal using LDH calcined at various temperatures (200 – 700 ^{o}C). It is obvious that dye removal percentage was highest with LDH calcined at 500 °C (CLDH500). Upon calcination, LDH was transformed to aluminium and magnesium oxides by the loss of interlayer anions, causing the adsorption of dye to increase in the temperature range 200 –500 °C, reaching the highest at 500 °C, corresponding to complete or almost complete decomposition of interlayer nitrate (Equation 6). Until this stage, the process was reversible; it was able to reconstruct its original LDH structure (memory effect) by incorporating anions such as water or anionic dyes or others (Equation 7). Above 500 °C, CLDH was transformed into a spinel which lost the property of reconstruction and reversibility, resulting in the observed decrease in dye adsorption. Other researchers using calcined Mg/Al-LDH to remove pollutants had also used the same temperature (500 °C) to obtain calcined LDH [16 – 18]. Based on this result, subsequent adsorption experiment was conducted using CLDH500.
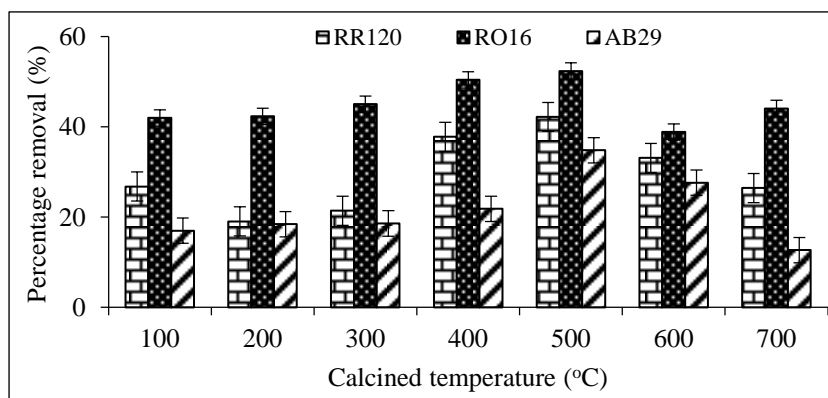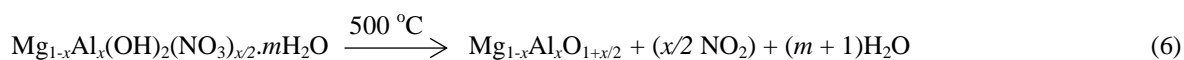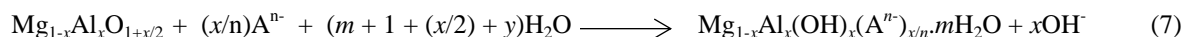

Figure 2. Percentage of dye removal by CLDHs calcined at different temperatures

Decomposition:

$$Mg_{1-x}Al_x(OH)_2(NO_3)_{x/2} \cdot mH_2O \xrightarrow{500\,^oC} Mg_{1-x}Al_xO_{1+x/2} + (x/2\ NO_2) + (m+1)H_2O \qquad (6)$$

Regeneration:

$$Mg_{1-x}Al_xO_{1+x/2} + (x/n)A^{n-} + (m + 1 + (x/2) + y)H_2O \longrightarrow Mg_{1-x}Al_x(OH)_x(A^{n-})_{x/n}.mH_2O + xOH^- \qquad (7)$$

Characterization of calcined and uncalcined LDH

X-Ray diffraction
The XRD pattern of precursor LDH in Figure 3(a) consists of three intense lines at low 2θ angle equivalent to diffraction by planes (003), (006) and (009) [7]. These sharp and symmetric peaks indicate the formation of a single well crystallized $MgAlNO_3$. The interlayer distance or (d_{003}) and (d_{006}) of LDHs corresponding to 8.01 Å and 3.99 Å, are due to basal reflections of crystal lattice, indicating successive layer stacking of the brucite-like lamellar sheets of hydrotalcite-like LDHs (ICSD collection code 086655). These values, together with other non- basal spacings at 1.54 Å (d_{110}) and 1.51 Å (d_{113}) are consistent with typical XRD pattern of LDH as reported by several authors [1, 3, 19 – 21]

Calcination up to 500 °C led to the progressive loss of physiosorbed water molecules, then the interlayer water and finally water from dehydroxylation of the brucite layer. The dehydration process was accompanied by the loss of interlayer anion leading to the collapse of the lamellar structure of LDH with the formation of mixed metal oxides $MgO-Al_2O_3$. As implied in the XRD pattern in Figure 3(b), the layered structure of the original LDHs has been destroyed in CLDH500 (CLDH) as evident from the significant absence of d_{006} and d_{003} peaks. Instead broad diffraction peaks appeared suggesting low structural order with almost total decomposition of the original LDHs with elimination of most interlayer nitrate anions and water. The XRD patterns of CLDH now resemble that of rock salt MgO whose reflection has shifted to higher angle due to the presence of Al^{3+} in in $Mg_{(1-x)}Al_xO_{(1+x/2)}$ [17]. No separated phases for Al^{3+} cations (Al_2O_3) were observed, indicating that these cations were dispersed in the MgO matrix solid solution [19], which is capable of being restored to LDH when rehydrated [5]. These observations were consistent with CLDH patterns cited in the literatures [1, 3, 17]. Figures 3(c – e) also shows that the diffraction patterns of dye- loaded CLDHs displaying peaks corresponding to (d_{003}) and (d_{006}) which are similar to the original LDH's XRD pattern. However the resulting peaks were broadened and with decreased peak intensity. This implies some reduction in crystallinity as a result of calcinations, rehydration and structural reconstruction which have occurred [21]. Due the 'memory effect', the CLDH was able to reconstruct and regain its original LDH when rehydrated [5].

After reconstruction, the basal spacings, notably (d_{003}) were observed to have increased in the dye-loaded CLDH (8.55 Å, 8.47 Å and 8.86 Å), indicating some increase in the interlayer distance. Theoretically, the increase in basal spacing (d_{003}) and (d_{006}) may indicate some dyes were intercalated into the spacing. Being bigger molecule than nitrate, the dye intercalated in the interlayer spacing was expected to result in an increase of the basal spacing or gallery height of the lamellar LDH. However, since the increase was not significantly large, it considered that total intercalation has indeed taken place [5]. The structural reconstruction property, called 'memory effect' forms the basis of regeneration for adsorbent LDH and the main mechanism of dye adsorption by CLDH though surface adsorption is presumed to have taken place as well [19]. This should be possible as surface area of calcined LDH has been reported to increase compared to its precursor LDH. On the basis of larger surface area of CLDH relative to LDH, it is fair to assume that CLDH offers better adsorption efficiency than its precursor.
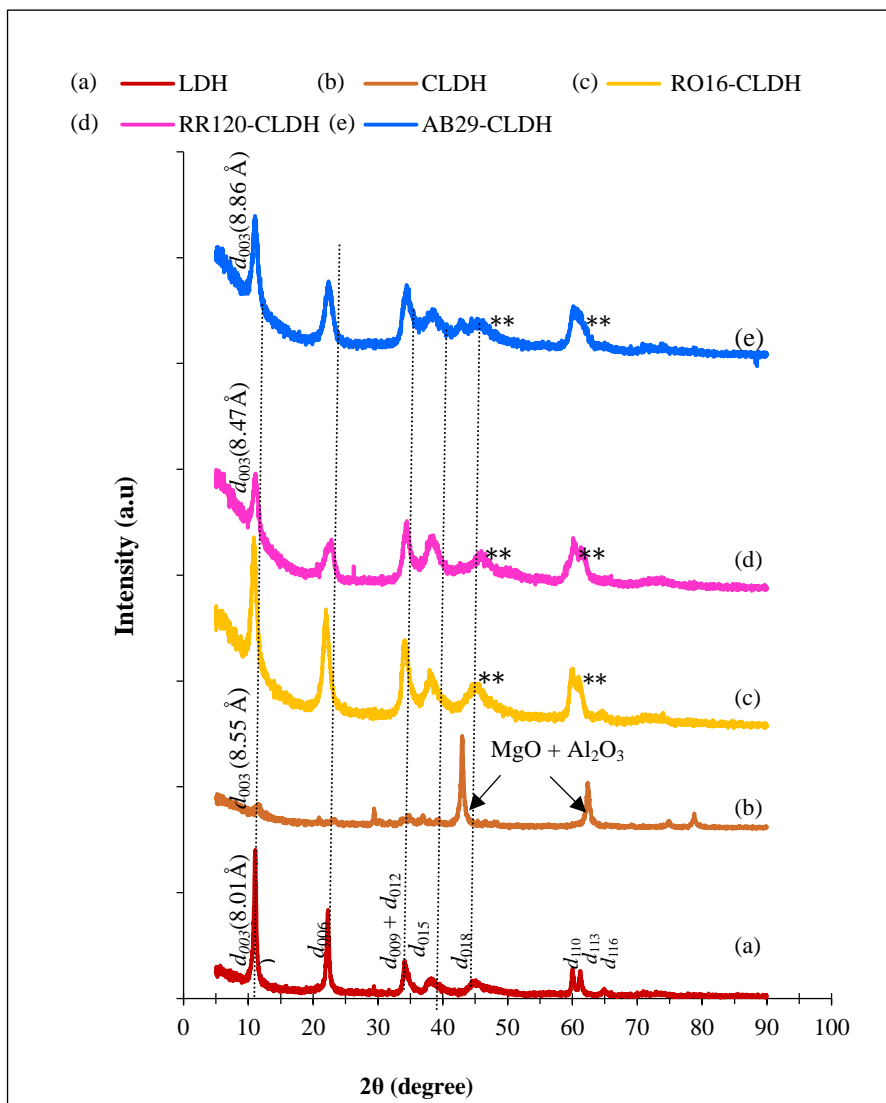
Figure 3. X-Ray Diffraction for LDH, CLDH and Dye loaded CLDH

Scanning electron microscopy

The textural properties of the LDH, CLDH and dye-loaded CLDHs have been investigated by scanning electron microscopy, as shown in Fig. 4 (a – e). It can be seen that the LDH image presents thin irregular aggregates of hexagonal platelets while CLDH resembles bigger platelets with rounded edges, with some still retaining the hexagonal-shaped of precursor LDH materials that were still retained in the CLDH product. This observation was understandable since both LDH and CLDH gave the same N_2 adsorption-desorption analysis results [21]. It has been reported that during thermal decomposition of LDH, the evolution of gas such as CO_2 (from carbonate) or NO/NO_2 (NO_x) from nitrate took place through fine pores at the brucite-like ($Mg(OH)_2$) layers, inducing the creation of channels and chimneys, which account for the increase surface area for calcined LDH. Since adsorption is a surface phenomenon, increase in surface area would enhance adsorption by CLDH. In the current study, the BET surface area for CLDH was found to be 121.58 m^2/g compared to 82.74 m^2/g for uncalcined LDH. Closer examination on SEM images in Fig.4 (a – e) reveals that dye materials have been incorporated onto the CLDH.
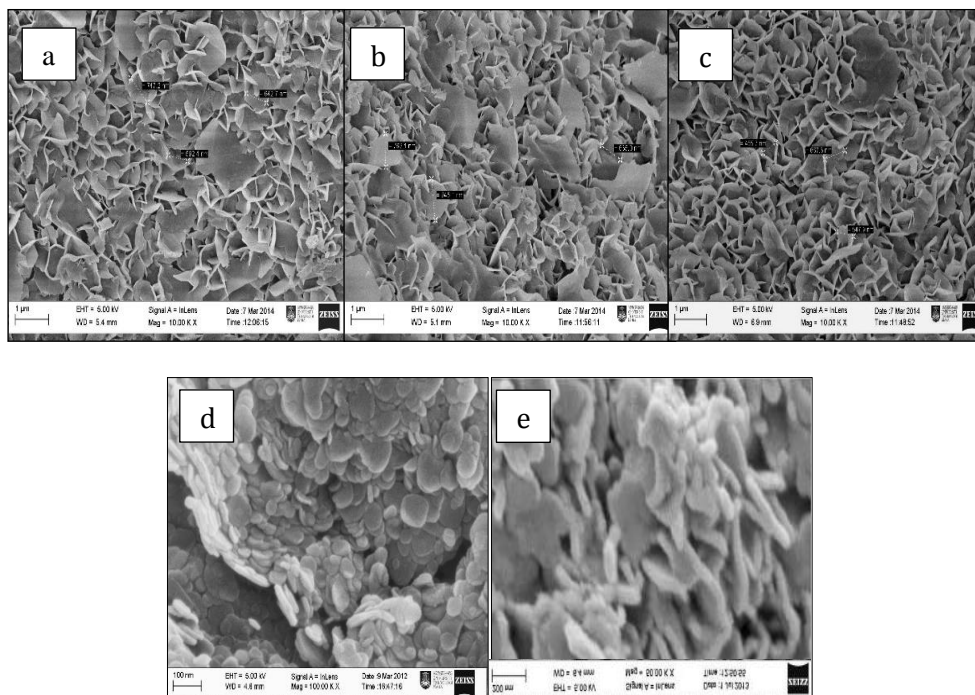
Figure 4. SEM images of (a) AB29-CLDH, Mag.:10K, (b) RO16-CLDH, Mag.:10 K, (c) RR120-CLDH, Mag.:10K, (d) LDH, Mag.: 100 K and (e) CLDH, Mag.: 50 K

Infrared spectra

The FTIR spectra of LDH, CLDH and dye-loaded CLDHs are presented in Figure 5. The LDH spectrum resembles that of other hydrotalcite-like phases with NO_3^- as the interlayer anions. The broad band at 3455 –3500 cm^{-1}, with a weak shoulder near 3100 cm^{-1} is due to the interlayer water molecules and the H-bonded stretching vibration respectively [7, 22, 23]. The weak peak at 1637 cm^{-1} may be assigned to the H_2O bending vibration of interlayer water, while the strong peak at 1384 cm^{-1} is attributed to the vibration of nitrate species. The bands in the range of 500 – 700 cm^{-1} are indicative of metal–oxygen–metal stretching [23].

Figure 5 shows the absorption bands of dye-loaded CLDH. It may be not plausible to exactly quantify the amount of NO_3^- the LDH or CLDH by FT-IR spectroscopy, but the reduced intensity of the nitrate peaks with reference to the broad band at 3450 cm^{-1} and at 1637 cm^{-1} after dye uptake indicate that anion exchange between NO_3^- ion and dye molecules did take place. The absorption band at around 1421 cm^{-1} in CLDH is indicative of the presence of CO_3^{2-} in the interlayer. The presence of CO_3^{2-} as an impurity may be difficult to avoid under the prevailing experimental conditions with the readiness of CLDH to take up moisture containing CO_2. The expected intercalation of dye in the CLDH interlayer may also be discerned by the presence of absorption band in the region around 1200 cm^{-1} which can be attributed to C-H bending vibration of aromatic dye molecules. The band occurring between 1450 cm^{-1} and 1380 cm^{-1} corresponds to the stretching mode of an azo-compound. The presence of sulfate S=O stretching vibration bands at around 1000 –1250 cm^{-1} and 1065 cm^{-1} due to sulfonic group in the dyes' structures were also observed. The result indicated that the dyes had existed on the surface of the CLDH after adsorption.
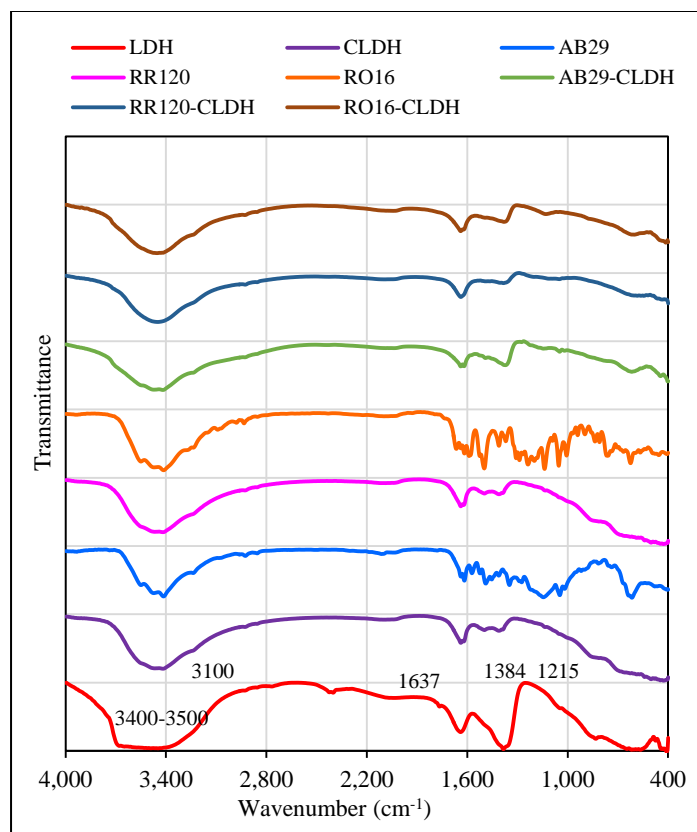
Figure 5. FTIR spectra of LDH, CLDH, dyes and dye-loaded CLDH, respectively

Effect of contact time and initial dye concentrations

The effect of contact time on and initial concentrations on dye removal by CLDH was compared with dye removal by LDH. The results for AB29, RO16 and RR120 are depicted in Figure 6 (a – c) for adsorption capacity, q_t, mg/g. Figure 6 shows that adsorption capacity increased with increased contact time until equilibrium was attained and thereafter remained almost unchanged after contact time of approximately 150 –180 min. For both LDH and CLDH, the adsorption capacity of dye increased rapidly within the first 10 – 20 min, after which the rate of adsorption decreased with time until it gradually approached a plateau due to the continuous decrease in the concentration driving force.

The time curves of dye removal for concentrations 50 – 100 mg/L in Figure 6 (a – c) are smooth and continuous indicating the possibility of a monolayer formation on adsorbent surface [16][23]. As Figure 6 (a – c) depict, the maximum adsorption capacity by CLDH and LDH decreased with increasing initial dye concentration as the number of moles of dye competing for the available surface area of the adsorbent which was fixed for a constant adsorbent dose, increased [16]. The most significant observation in this experiment was the enhanced dye uptake, both in terms of percentage dye removal and adsorption capacity by CLDH over its precursor LDH for any given initial dye concentration. Examples of this elevated dye removal by CLDH over its precursor LDH are highlighted for 50 and 100 mg/L dye concentration for AB29, RO16 and RR120 in Table 1, which shows the values of q_t (mg/g). Calculation for (dye uptake by CLDH/dye uptake by LDH) ratio reveals that the increase was between 150 – 200 %. The increase uptake by CLDH was attributed largely to the 'memory effect' phenomenon which is synonym with structural reconstruction by calcined LDH to its original layered structure when exposed to aqueous solution containing ions such as simple inorganic ions (eg. CO_3^{2-}, SO_4^{2-}, SeO_3^{2-}, CO_3^{2-}, NO_3^-, Cl^-) or polar organic molecules [5]. Among the three dyes, AB29 exhibit the highest dye uptake followed by RO16 and RR120, the same

trend as uptake by pristine LDH. This trend is reflective of binding capacity of these dyes towards the adsorbent LDH and CLDH.
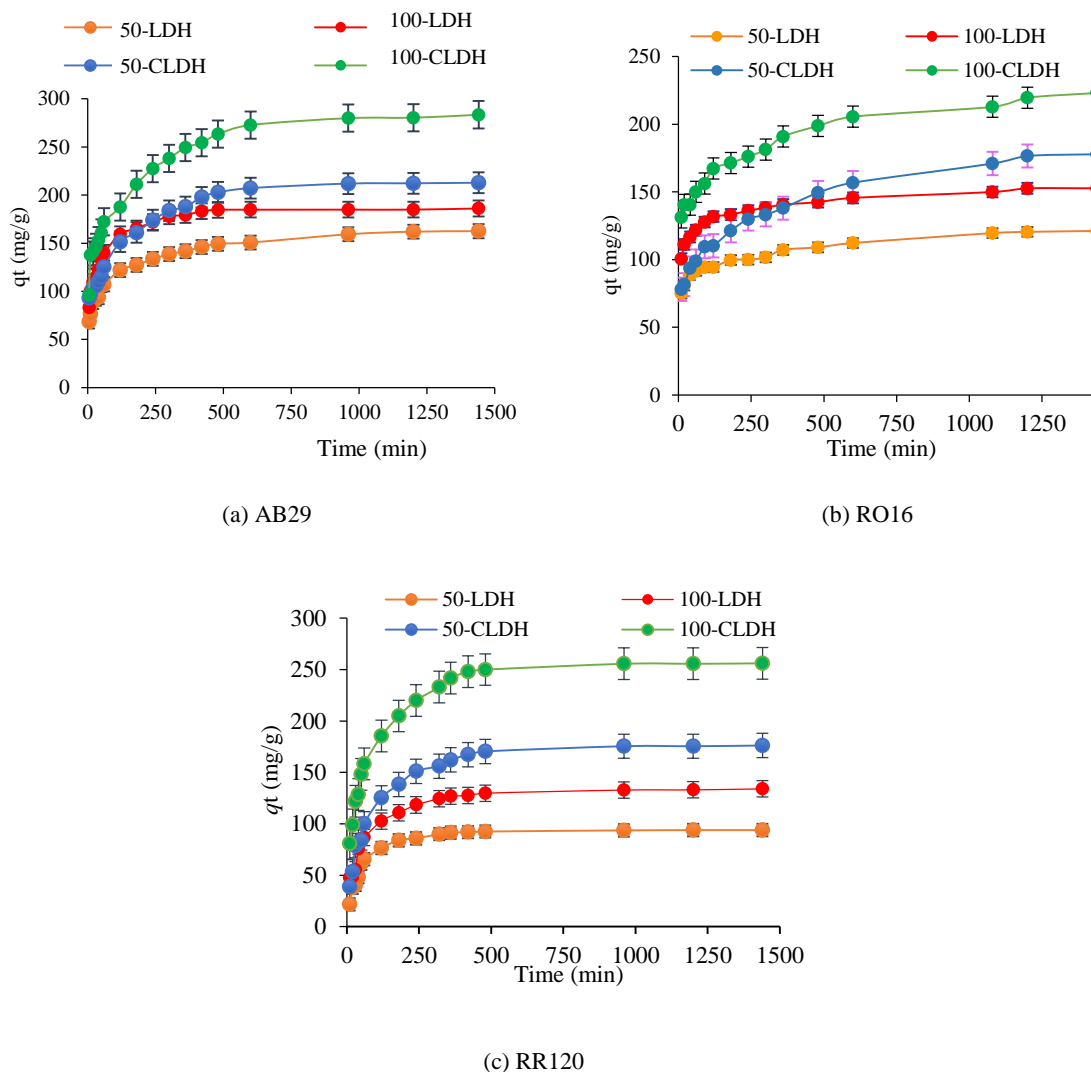

(a) AB29

(b) RO16

(c) RR120

Figure 6. Effect of contact time and initial dye concentrations on adsorption capacity in adsorption by LDH and CLDH on anionic dyes (a)AB29, (b) RO16 and (c) RR120

Kinetic of adsorption

The kinetic parameters for PFO, PSO and IPD kinetic models for dye-LDH and dye-CLDH obtained using experimental data for Figure 6 are summarised in Tables 2, 3 and 4, respectively. It is apparent that the values of correlation coefficient (R^2) are mostly quite high (> 0.9) for PFO, PSO and IPD models. Based on the correlation coefficient (R^2), it can be seen that PSO have better fitting ($R^2 = 0.99 - 1.00$) than PFO ($R^2 = 0.85 - 0.99$). Furthermore the values of q_e calculated ($q_{e,alc}$) from PSO model are more consistent with the experimental q_e ($q_{e,expt.}$), indicating that the experimental kinetic data for AB29, RO16 and RR120 adsorption by LDH and CLDH are suitable for this model. Similar finding was obtained by [17] on Reactive Orange 10 adsorption by CLDH. In addition, the values of ($q_{e,\ calc}$) and q_e ($q_{e,expt.}$) shows that maximum adsorption capacities are higher for CLDH than

those by LDH. The results are consistent with CLDH being a more efficient adsorbent than LDH as dye scavenger from solution. The order of adsorption affinity for adsorbent is reflected from the values of the adsorption capacities. It can be seen that the order of affinity of adsorbent for dyes under study is AB29 >RO16 > RR120. This trend was obeyed by systems, dye-LDH and dye-CLDH.

Table 1. Comparison between dye uptake by LDH and CLDH in terms of adsorption capacity, ($q_{t,expt}$) at t=24 h, T=25 ^{o}C, W/V=0.2g/L for AB29, RO16 and RR120, respectively

Dye	Adsorbent	Concentration	
		50 mg/L	100 mg/L
		qt (mg/g)	qt (mg/g)
AB29	LDH	162.501	186.100
	CLDH	212.830	283.506
RO16	LDH	121.160	152.655
	CLDH	177.858	268.140
RR120	LDH	96.338	133.979
	CLDH	176.155	256.074

To understand this trend, factors that influence dye binding capacity to adsorbent have to be considered. These factors include the characteristics and chemistry of the dye such as molecule structure, molecular weight, spatial and steric effect, all of which exert influence on the adsorption onto adsorbent either singly or in concert with other factors present in the aqueous environment. In this case AB9 and RO16, having smaller size than RR120 would be more unhindered during adsorption compared to the bulkier RR120 in terms of spatial and steric effect, even though RR120 has six sulfonic groups (SO_3^-) compared to two in AB29 and RO16. As a result RR120 would have less mobility in attaching itself to adsorbent, even though the sulfonic groups render negative charge to the RR120, thus enhancing the dye ability to attach itself onto positively-charged adsorbent. In terms of negative charges, AB29 would be expected to have similar binding capacity. The fact that acid dye AB29 displayed better binding capacity than vinylsulphone reactive dye RO16 is probably due to a side reaction of RO16 in water. The vinylsulphone group ($-CH_2CH_2SO_2$ -) in RO16 is electron attracting group which induces electron deficiency on the terminal carbon atom, initiating a nucleophilic (addition reaction) attack by electron rich hydroxyl ion, OH^- from water. This hydrolysis can be represented by the reaction:

$$Dye\text{-}SO_2CH = CH_2 + H\text{-}OH \longrightarrow Dye\text{-}SO_2\text{-}CH_2\text{-}CH2\text{-}OH \tag{8}$$

As a result of this hydrolysis, RO16 is less available for binding sites on LDH/CLDH with an overall reduction in binding capacity of RO16.

The resulting IPD linear plots of q_t versus $t^{0.5}$ (not shown) show the existence of two or three-staged linear curves, none of which pass through the origin. This is an indication that IPD was not the sole rate limiting step. Moreover, the existence a two or three-linear phases for each concentration implies that most likely the adsorption process involved more than one rate equation.

Table 2. Pseudo-first order and pseudo-second-order kinetic parameters for dye-LDH system for AB29, RO16 and RR120, W/V= 0.2 g/L, T=25°C

AB29-LDH			Pseudo first-order			Pseudo second-order			
Co (mg/L)	$q_{e,expt.}$ (mg/g)	$q_{e, calc.}$ (mg/g)	$k_{1} \times 10^{-3}$ (1/min)	$h_{1} \times 10^{-1}$ (mg/g.min)	R^2	$q_{e, calc.}$ (mg/g)	$k_{2} \times 10^{-4}$ (mg/g min)	h_{2} (mg/g.min)	R^2
50	162.500	122.462	4.836	5.923	0.988	156.250	1.74	5.970	0.998
100	186.100	156.315	4.145	6.480	0.990	188.679	3.17	11.274	0.994
RO16-LDH			First-order kinetic			Second-order kinetic			
Co (mg/L)	$q_{e,expt.}$ (mg/g)	$q_{e, calc.}$ (mg/g)	$k_{1} \times 10^{-3}$ (1/min)	$h_{1} \times 10^{-3}$ (mg/g.min)	R^2	$q_{e, calc.}$ (mg/g)	$k_{2} \times 10^{-4}$ (mg/g min)	h_{2} mg/g.min	R^2
50	121.160	18.621	2.764	2.533	0.944	106.383	6.38	7.225	0.992
100	152.655	35.278	2.533	2.764	0.946	185.185	3.36	11.534	0.999
RR120-LDH			First-order kinetic			Second-order kinetic			
C_{o} (mg/L)	$q_{e,expt.}$ (mg/g)	$q_{e, calc.}$ (mg/g)	$k_{1} \times 10^{-3}$ (1/min)	$h_{1} \times 10^{-1}$ (mg/g.min)	R^2	$q_{e, calc.}$ (mg/g)	$k_{2} \times 10^{-4}$ (g/mg min)	$h_{2} \times 10^{-3}$ (mg/g min)	R^2
50	96.338	57.610	8.291	4.78	0.982	96.154	3.553	3.286	1.000
100	133.979	79.177	6.448	5.11	0.983	136.986	2.132	4.002	1.000

Table 3. Pseudo-first order and pseudo-second-order kinetic parameters for dye-CLDH system for AB29, RO16 and RR120, W/V = 0.2 g/L, T = 25 ^{o}C

AB29-CLDH			Pseudo first-order			Pseudo second-order			
Co (mg/L)	$q_{e,expt.}$ (mg/g)	$q_{e, calc.}$ (mg/g)	$k_{1} \times 10^{-3}$ (1/min)	$h_{1} \times 10^{-1}$ (mg/g.min)	R^2	$q_{e, calc.}$ (mg/g)	$k_{2} \times 10^{-5}$ (g/mg min)	h_{2} (mg/g min)	R^2
50	212.83	103.514	4.606	5.719	0.946	250.000	8.84	5.525	0.998
100	283.506	141.254	2.303	3.253	0.991	333.333	6.34	7.042	0.998
RO16-CLDH			Pseudo first- order			Pseudo second-order			
Co (mg/L)	$q_{e,expt.}$ (mg/g)	$q_{e, calc.}$ (mg/g)	$k_{1} \times 10^{-3}$ (1/min)	$h_{1} \times 10^{-1}$ (mg/g.min)	R^2	$q_{e, calc.}$ (mg/g)	$k_{2} \times 10^{-5}$ (g/mg min)	$h_{2} \times 10^{-3}$ (mg/g min)	R^2
50	177.858	105.196	3.224	2.423	0.965	181.818	7.944	2.631	0.994
100	268.140	111.764	3.224	3.603	0.958	277.778	7.840	6.050	0.999
RR120-CLDH			Pseudo first-order			Pseudo second-order			
Co (mg/L)	$q_{e,expt.}$ (mg/g)	$q_{e, calc.}$ (mg/g)	$k_{1} \times 10^{-3}$ (1/min)	h_{1} (mg/g.min)	R^2	$q_{e, calc.}$ (mg/g)	$k_{2} \times 10\text{-}10^{-4}$ (g/mg min)	$h_{2} \times$ (mg/g min)	R^2
50	176.155	97.275	4.376	0.4256	0.938	181.818	3.6	3.824	1.000
100	256.074	168.578	6.909	1.1647	0.992	344.828	0.58	11.136	1.000

The calculated values of IPD rate constant, k_{p}, C and the R^2 values summarized in Table 4 were obtained through fitting the experimenal data at second linear portion of Equation (3)[24]. The correlation coefficients for IPD diffusion model obtained are between 0.746 and 0.979. The R^2-values are quite high and some are close to unity

788

indicating the validity of application of this model. The values of IPD rate constant, k_p decreased with decreasing initial dye concentration which provided the driving force in overcoming the resistance due to mass transfer [24] and was found to be correlated with the initial dye concentration. The values of *C* give an idea about the thickness of the boundary layer, i.e. the larger the intercept the greater is the boundary layer effect (mass resistance), and the greater is the contribution of the surface adsorption in the rate limiting step[25]. In conclusion the adsorption mechanism of dye uptake by LDH is quite a complex process and cannot be explained by a single kinetic model alone, but could have involved more than single type of kinetic mechanism, all of which may be operating simultaneously [26][27].

Table 4. Intraparticle diffusion constants at different initial dye concentrations at 25 ^{o}C for dye-LDH and dye-CLDH system for AB29, RO16 and RR120; W/V = 0.2 g/L, T = 25°C

Dye		Intraparticle diffusion model			Dye		Intraparticle diffusion model		
LDH	C_o mg/L	k_p (mg/g.min$^{0.5}$)	C	R^2	CLDH	C_o mg/L	k_p (mg/g.min$^{0.5}$)	C	R^2
AB29	50	1.710	107.401	0.892	AB29	50	4.396	104.172	0.983
	100	1.333	151.071	0.746		100	6.209	127.031	0.974
RO16	50	0.4251	91.001	0.955	RO16	50	2.929	77.801	0.965
	100	0.8052	123.98	0.973		100	2.643	132.03	0.952
RR120	50	2.608	83.250	0.985	RR120	50	4.095	83.252	0.979
	100	2.302	77.438	0.957		100	6.073	122.76	0.978

Mechanisms of adsorption by CLDH
Results on dye removal had shown that CLDH exhibited better efficiency than its precursor LDH in removing anionic dyes from solution. The resulting calcined LDH (CLDH) has higher specific surface areas compared to its precursor LDH. Since adsorption is a surface phenomenon, this could be a major factor accounting for the significant increase in the anionic dye affinity for CLDH. During calcination process, fine pores and channels were generated as H_2O vapor and NO_2/NO gas were evolved, resulting in the creation of chimneys and channels in the particles, which ultimately resulted in the increase in specific surface area and smaller pores in the mesoporous CLDH particles.

The diffactograms of calcined materials shown in Figure 3 show that the CLDH displayed its 'memory effect' by reconstructing to its former LDH structure as evident through the re-emergence of (003) and (006) reflections. This is further supported by the observed of somewhat broadened, less symmetrical peaks with reduced intensity in comparison to the original LDH, indicating less ordered platelet–like structure and crystallinity [5], typical of post adsorption products following rehydration and reconstruction. It has been postulated that intercalation via reconstruction had played a role in this process of adsorption by CLDH according to Eq. (8), given the relatively slow increase in dye adsorption as dye concentration was increased (Figure 6). This 'memory effect' may be construed as a reconstruction reaction expressed as expressed by the preceding Equation (8) [21].

It may be concluded that under prevailing conditions, external surface adsorption appeared to be the main mechanism in the adsorption. Furthermore, the peaks corresponding to MgO in CLDH still remained in all CLDH products, indicating that   reconstruction was not complete.

Regeneration and recyclability
Regeneration of adsorbent for possible reuse gives an advantage commercially and economically to an adsorbent. The results from four cycles of regeneration were obtained from calcination-hydration process whereby the adsorbed dyes was combusted during calcination, followed by rehydration of the regenerated adsorbent LDH in the

dye solution.   As shown in Figure 7, the thermally treated   LDHs, exhibited progressive loss in percentage dye removal after each cycle. This percentage loss varied for each dye. After four cycles the efficiency has been reduced to almost 10 – 25 %, and may be regarded as uneconomical for further regeneration. A possible reason for the reduced efficiency is the reduced crystallinity of adsorbent, after undergoing repeated calcination-hydration process [28].
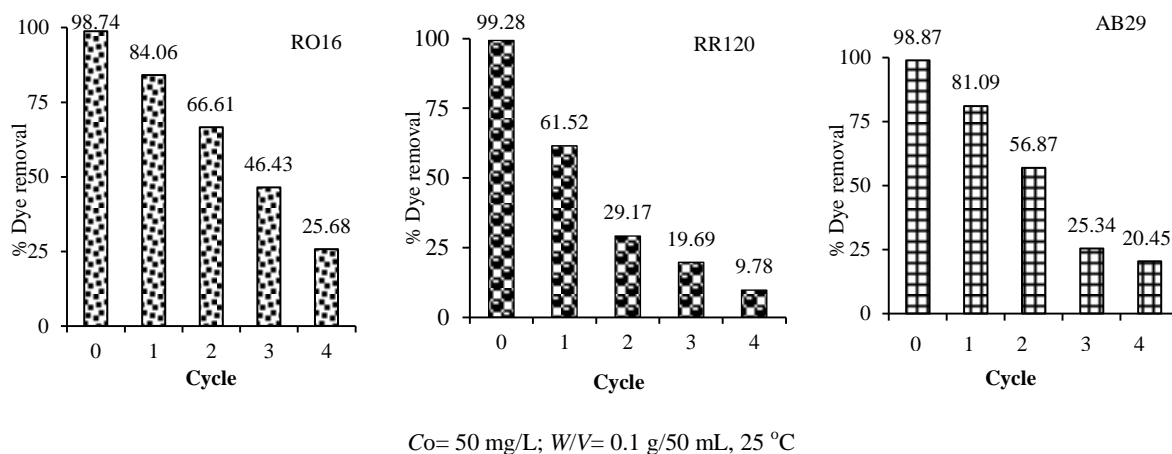

Co= 50 mg/L; W/V= 0.1 g/50 mL, 25 ^{o}C

Figure 7. Regeneration of CLDH after adsorption by RO16, RR120 and AB29

Conclusion

The adsorption of AB29, RO16 and RR120 was much more efficient by CLDHs than LDHs. Similarly, the adsorption capacities of CLDHs were much higher than that of its precursor LDHs. The affinity towards dye removal follows the order: AB29 > RO16 > RR120. Therefore CLDHs may be recommended for use in sequestering higher concentration of anionic dyes, while LDHs may be more appropriately used for low concentrations. The kinetics of adsorption of anionic dyes was well described by PSO reaction while PFO reaction and IPD kinetics may have contributed to the overall mechanism of dye uptake. Reconstruction of LDH via rehydration and intercalation was evident from X-ray diffraction and FTIR spectroscopy analysis. Recycling and reuse of LDH/CLDH was possible, until the fourth cycle when this is no longer economical. For better performance, only the second and third cycle may be considered when the percentage dye removal could still be maintained at 50 – 66 % for these dyes.

References

1.   El Gaini, L. Lakraimi, M., Sebbar, E., Meghea, A., and Bakasse, M. (2009). Removal of indigo carmine dye from water to Mg–Al–CO3-calcined layered double hydroxides. *Journal of Hazardous Materials*, 161: 627 – 632.

2.   Lazaridis, N. K., Karapantsios, T. D. and Georgantas, D. (2003). Kinetic analysis for the removal of a reactive dye from aqueous solution onto hydrotalcite by adsorption. *Water Research*, 37: 3023 – 3033.

3.   Abdelkader, N. B-H., Bentouami, A. Derriche, Z., Bettahara, N., de Menorval, L-C. Chemical. (2011). Synthesis and characterization of Mg–Fe layer double hydroxides and its application on adsorption of Orange G from aqueous solution. *Engineering Journal*, 169: 231 – 238.

4.   Das, J., Das, D. K. M. and Parida, K. M. (2006). Preparation and characterization of Mg–Al hydrotalcite-like compounds containing cerium, *Journal of Colloid and Interface Science*, 301: 569 –574.

5.   Auxilio, A. R., Andrews, P. C., Junk, P. C. and Spiccia, L. (2009). The adsorption behavior of C.I. Acid Blue 9 onto calcined Mg–Al layered double hydroxides. *Dyes and Pigments*, 81: 103 – 112.

6. Das, J., Das, D. K. M. and Parida, K. M. (2006). Preparation and characterization of Mg–Al hydrotalcite-like compounds containing cerium, *Journal of Colloid and Interface Science*, 301: 569 –574.

7. Lagergren, S. (1898). About the theory of so called adsorption of soluble substances. K. Sven. Vetenskapsakad. Handl., Band 24, 1 – 39.

8. Ho, Y. S. (2006). Review of second-order models for adsorption systems. *Journal of Hazardous Materials*, 136: 681 – 689.

9. Weber, W. J. and Morris, J. C. (1963). Kinetics of Adsorption on Carbon from Solution. *Journal of the Sanitary Engineering Division*, 89(2): 31 – 60.

10. Reichle, W. T. (1986). Synthesis of anionic clay minerals (mixed metal hydroxides, hydrotalcite). *Solid State Ionics*, 22: 135 – 141.

11. Forano, C., Hibino, T., Lerouxa, F. C. and Taviot-Gue, H. (2006). Layered double hydroxides. *Developments in Clay Science*, 1: 1021 – 1095.

12. Kameda, T., Yamazaki, T. and Yoshioka, T. (2009). Preparation of MgAl layered double hydroxide intercalated with 2,7-Naphthalene Disulfonate and its selective uptake of aromatic compounds from aqueous solutions. *Bulletin of the Chemical Society of Japan*, 82: 1436 – 1440.

13. Mahmoodi, N. M., Hayati, B. and Arami, M. (2012). Kinetic, equilibrium and thermodynamic studies of ternary system dye removal using a biopolymer. *Industrial Crops and Products*, 35: 295 – 301.

14. Senthilkumaar, S., Kalaamani, P., Porkodi, K., Varadarajan, P. R. and Subburaam, C. V. (2006). Adsorption of dissolved reactive red dye from aqueous phase onto activated carbon prepared from agricultural waste. *Bioresource Technology*, 97: 1618 – 1625.

15. Yu, L. and Luo, Y. (2014). The adsorption mechanism of anionic and cationic dyes by Jerusalem artichoke stalk-based mesoporous activated carbon. *Journal of Environmental Chemical Engineering*, 2: 220 – 229.

16. Das, J., Das, D. K. M. and Parida, K. M. (2006). Preparation and characterization of Mg–Al hydrotalcite-like compounds containing cerium. *Journal of Colloid and Interface Science*, 301: 569 –574.

17. Bouhent, M. M., Derriche, Z., Denoyel, R., Prevot, V., and Forano, C. (2011). Thermodynamical and structural insights of orange II adsorption by MgRAlNO3 layered double hydroxides. *Journal of Solid State Chemistry,* 184: 1016 – 1024.

18. Bouraada, M., Belhalfaoui, F. and Ouali, M. S. (2009). Sorption study of an acid dye from an aqueous solution on modified Mg–Al layered double hydroxides. *Journal of Hazardous Materials*, 163: 463 –467.

19. Extremera, R., Pavlovic, I., Pérez, M. R., and Barriga, C. (2012). Removal of acid orange 10 by calcined Mg/Al layered double hydroxides from water and recovery of the adsorbed dye. *Chemical Engineering Journal*, 213: 392 – 400.

20. Zhu, M-X., Li, Y-P., Xie, M. and Xin, H-Z. (2005). Sorption of an anionic dye by uncalcined and calcined layered double hydroxides: A case study. *Journal of Hazardous Materials*, 120: 163 – 171.

21. Ni, Z. M., Xia, S. J., Wang, L. G., Xing, F. F. and Pan, G. X. (2007). Treatment of methyl orange by calcined layered double hydroxides in aqueous solution: Adsorption property and kinetic studies. *Journal of Colloid and Interface Science*, 316: 284 – 291.

22. Crepaldi, E. L., Tronto, J., Cardoso, L. P. and Valim, J. B. (2002). Sorption of terephthalate anions by calcined and uncalcined hydrotalcite-like compounds. *Colloids and Surfaces A: Physicochemical and Engineering Aspects*, 211: 103 –114.

23. Ferreira, O. P., Alves, O. L., Gouveia, D. X., Filho, A. G. S., de Paiva, J. A. C. and Filho, J. M. (2004). Thermal decomposition and structural reconstruction effect on Mg–Fe-based hydrotalcite compounds. *Journal of Solid State Chemistry*, 177: 3058 – 3069.

24. Naveen, N., Saravanan, P., Baskar, G. and Sahadevan, R. (2011). Equilibrium and kinetic modeling on the removal of Reactive Red 120 using positively charged Hydrilla verticillata. *Journal of the Taiwan Institute of Chemical Engineers*, 42: 463 – 469.

25. Kobiraj, R., Gupta, N., Kushwaha, A. K. and Chattophadhyaya, M. C. (2012). Determination of equilibrium, kinetic and thermodynamic parameters for the adsorption of the brilliant green dye from aqueous solutions onto eggshell powder. *Indian Journal of Chemical Technology*, 20: 26 – 31.

26. Greluk, M. and Hubicki, Z. (2010).Kinetics, isotherm and thermodynamic studies of Reactive Black 5 removal by acid acrylic resins. *Chemical Engineering Journal* 162: 919 – 926.

27. Baccar, R., Blánquez, P., Bouzid, J., Feki, M., Attiya, H. and Sarrà, M. (2013).   Modelling of adsorption isotherms and kinetics of a tannery dye onto an carbon prepared from an agricultural by-product activated carbon prepared from an agricultural by-product. *Fuel Processing Technology*, 106: 408 – 415.
28. Ulibarri, M. A., Pavlovic, I.. Barriga, C. Hermos´ın and Cornejo, M. C. (2001). Adsorption of anionic species on hydrotalcite-like compounds: effect of interlayer anion and crystallinity, *Applied Clay Science*, 18: 17 – 27.